ICAS 2016
30th Congress of the International Council of the Aeronautical Sciences
DCC, Daejeon, Korea ; September 25-30, 2016

COLLABORATIVE MULTI-LEVEL MDO PROCESS DEVELOPMENT AND APPLICATION TO LONG-RANGE TRANSPORT AIRCRAFT

Stefan Görtz*, Časlav Ilić*, Mohammed Abu-Zurayk*, René Liepelt*, Jonas Jepsen*, Tanja Führer*, Richard Becker*, Julian Scherer*, Thiemo Kier*, Martin Siggel*
***German Aerospace Center (DLR)**

Abstract

DLR's work on developing a distributed collaborative MDO environment is presented. A multi-level approach combining high-fidelity MDA for aerodynamics and structures with conceptual aircraft design methods is employed. Configuration-specific critical loads are evaluated and used for sizing the structure. A gradient-free optimization algorithm is used to optimize the fuel burn of a generic long-range wide-body transport aircraft configuration with 9 shape parameters. First results show a truly multidisciplinary improvement of the modified design. The result of a gradient-free high-fidelity MDO with preselected load cases and five shape parameters is also presented, comparing a full mission analysis with results for the Breguet range equation. Finally, a gradient-based high-fidelity aero-structural optimization subject to 7 pre-selected load cases is performed for a wing-body configuration that is parametrized by 360 freeform deformation design variables for the aerodynamic shape and 348 thickness design variables for the internal structure, resulting in a 6% increase in the objective function.

1 Introduction

There is a growing need in industry to shorten the time required to design new aircraft. The next generation of civil transport aircraft is likely to feature innovative designs for which little design experience has been accumulated so far. Thus, being able to reliably assess and make use of the potential of new technologies by performing trade-off studies and to estimate their impact in terms of, for example, weight, fuel burn or environmental impact will be crucial. This requires the use of highly accurate, high-fidelity numerical methods that capture the relevant physics as complex multidisciplinary interactions may occur that cannot be evaluated by low-fidelity models.

To address this need for an advanced design capability, DLR is engaged in the development of a distributed multidisciplinary optimization (MDO) environment based on disciplinary methods and tools from low to high fidelity. This collaborative MDO platform is to provide a robust, integrated design process for aerodynamics and structures, while taking the engine into account. It is to be used to design long-range wide-body transonic transport aircraft considering relevant constraints.

These MDO activities, which are part of the DLR-project Digital-X [4], are based on previous MDO experience: MDO capabilities at the preliminary design level were originally developed in the DLR-projects TIVA I/II [1] and VAMP [2]. Initial MDO work based on high-fidelity numerical methods took place in the DLR project MDOrmec [3].

In order to use the full potential of multidisciplinary design the idea is to replace the predominantly sequential approach to detailed design by pursuing a multi-levelapproach, which combines highly accurate multidisciplinary analysis (MDA) processes for aerodynamics and structures with simplified and rule-based design techniques for conceptual aircraft design and a fast integrated loads process for identifying configuration-specific critical load cases. Coupling of the individual tools and components, which are installed locally on different computers at eight different DLR institutes and labs at six different sites all over Germany, and execution of the overall process chain is controlled by DLR's workflow

management tool RCE (Remote Component Environment) [6]. The high-fidelity MDA tools are coupled and executed on an HPC cluster system using DLR's parallel simulation environment FlowSimulator [5]. The description of the aircraft geometry and the exchange of data between components are achieved using DLR's XML-based Common Parametric Aircraft Configuration Scheme (CPACS) [7]. The aircraft geometry is modeled using DLR's geometry library TIGL and various tool-specific model generators which are able to read and write the CPACS data format.

The paper is organized as follows: the Airbus XRF-1 long-rage transport aircraft configuration that is used as a baseline and reference throughout is described in the next paragraph. Then we describe the collaborative MDO environment which is based on more than 40 disciplinary tools from low- to high-fidelity. Next, we present the setup of a gradient-free optimization of the XRF-1 using this complex multi-level MDO process and show preliminary results. Thereafter, we present first results that were achieved with the same MDO chain but with reduced complexity by only considering the high-fidelity disciplinary tools. We present results of a gradient-free followed and a gradient-based optimization of the XRF-1.

2 Reference aircraft description

The Airbus XRF-1 transport aircraft configuration is used as the reference geometry in the following to demonstrate the capabilities of the different MDO approaches. The XRF-1 is a generic research configuration similar to an existing Airbus wide-body aircraft.

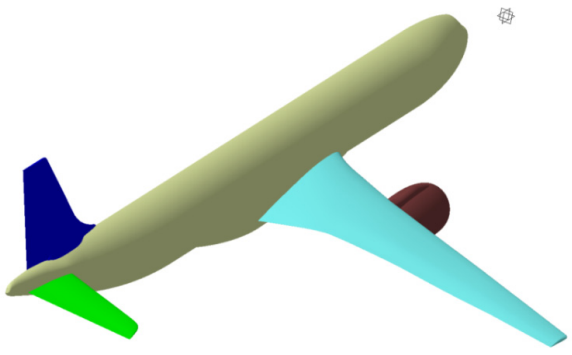

Fig. 1. XRF-1 generic long-range transport aircraft used as a baseline for MDO

Fig. 1 shows the baseline XRF-1 geometry, which is wing/fuselage/tail configuration. It was specified consistently in CPACS format and a simplified 8,000 nm mission consisting of climb, cruise, descent and landing as well as a flight to an alternate airport (200 nm). As no payload-range diagram and Top-Level Aircraft Requirements (TLARs) were available for the XRF-1, they were reconstructed with the help of DLR's preliminary design tools. Adjustments were done where necessary to create a consistent data set. A selection of the reconstructed TLARs is given in Table 1. The TLAR were validated by performing a simulation of the reference long-range mission with the preliminary design tools, showing good agreement with Airbus reference data for this mission.

TLAR	Value
Design range [nm]	5600
Max. range@MTOW [nm]	≥8000
Cruise alt [ft]	35000
Cruise Mach number	0.83
PAX #	353
Max. payload	≥48t
Max. take-off thrust/engine [kN]	334.7
Take-off field length	≤2700m

Table 1: Reconstructed TLAR (selection)

3 MDO architecture and process chain

Fig. 2 schematically shows the sequential MDO process chain that has been developed within the DLR project Digital-X. The formulation is considered a per-cycle (and per level) "multidisciplinary feasible" (MDF) approach, coupling the involved disciplines at different stages of fidelity. The process is driven by a single, gradient-free optimization algorithm, where all objective-relevant data are provided by the detailed level (i.e., coupled high-fidelity methods).

Although there are several options to arrange the different levels and disciplines, in the Digital-X project we made a deliberate choice to pursue a sequential multi-level MDF approach. This may be considered a natural choice to take the first step towards MDO as it

is easy to implement despite the complexity involved. Also, this approach is close to industrial processes, which tend to be rather sequential. Finally, this implementation may act as a reference for other, more advanced approaches, see the gradient-based high-fidelity MDO at the end of this paper, for example.

The chosen multi-level/multi-fidelity MDO approach allows for an efficient treatment of configurational design requirements by means of preliminary design methods that update dependent aircraft parameters after a change of the design variables and check the feasibility of the configuration. Assessment of configuration-specific critical load cases and initial structural sizing is done in the second stage. High-fidelity coupled CFD/CSM (computational fluid dynamics/computational structural mechanics) simulations and refined structural sizing are employed at the detailed level to provide the required performance and mass data for mission analysis and objective function evaluation.

This automated process chain has been implemented in DLR's distributed software integration environment RCE and heavily relies on the aircraft description in CPACS format.

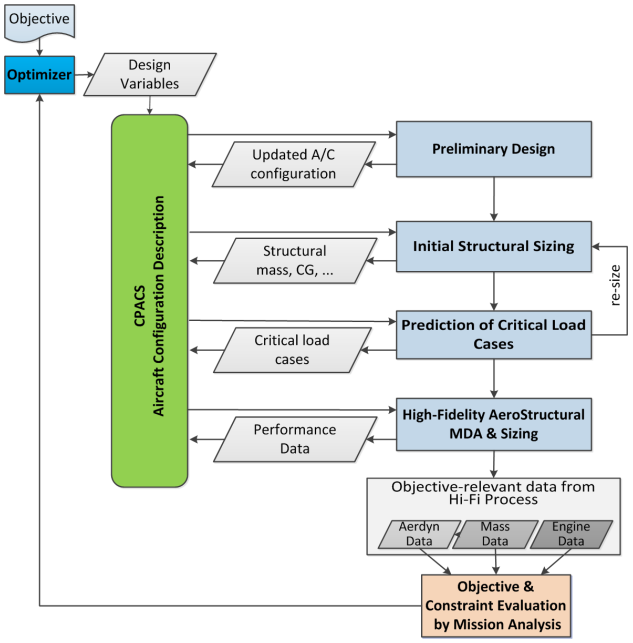

Fig. 2. Multi-level/multi-fidelity MDO process chain (schematic)

4 Gradient-Free Multi-Level MDO

The process chain shown in Fig. 2 works as follows:

The optimizer issues a new set of wing design variables, based on which the initial update of the CPACS data set is performed. This leaves some of the dependent parts of the CPACS data set in an inconsistent state, with respect to the constraints that the design should satisfy. The optimization algorithm is a subplex, a gradient-free method that performs a series of incomplete simplex optimizations by subspaces of design parameters.

This data set is sent to the preliminary design, where the horizontal and vertical tail sizes, as well as the wing position, are adjusted to reach the desired stability and controllability criteria. Then the preliminary overall aircraft synthesis is performed, to determine the component masses. Some of these masses may be used as initial guesses for methods later in the process, and some (such as secondary structure masses) are used as is. Also various design constraints, such as ferry range and takeoff/landing distance are computed here, although at the moment they are ignored by the optimizer. The main disciplinary tools used here are VAMPzero [8],[9] for initial empirical/statistical synthesis, a vortex-lattice aerodynamics code, and tools for estimating zero-lift drag, for physics-based mass estimation, and for mission evaluation.

The next part of the process is initial structure sizing and prediction and evaluation of critical load cases. Based on the updated geometry, the structural dynamic master model (DMM) of the XRF-1 shown in Fig. 3 is created from CPACS and thousands of load cases are evaluated using a fast doublet-lattice method (DLM) with compressibility corrections and corresponding grid, see Fig. 3 (bottom), and a few tens of load cases are selected as critical. A simplified structure model (beam elements and condensed masses), see Fig. 3 (top), is sized by the critical loads, and the new sized model is used for the next load evaluation and selection step. This is repeated until the structural mass converges. The two main disciplinary tools used here are MONA [10] for dynamic structural

model generation and sizing and Varloads [11],[12] for load case evaluation and selection. NASTRAN is used here as the structural solver.

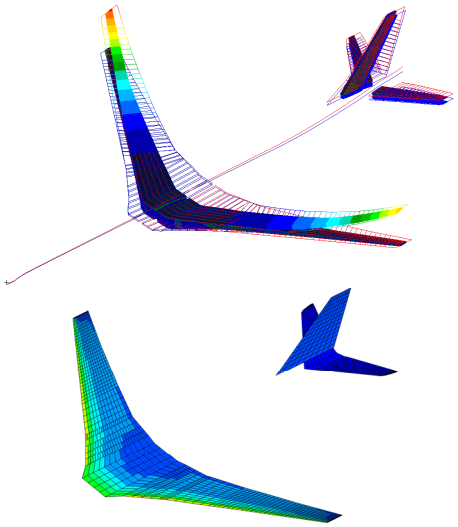

Fig. 3. Dynamic XRF-1 model (top: global FEM model for modal analysis; bottom: doublet lattice model with pressure distribution)

The final part of the process is high-fidelity sizing and performance evaluation. The final set of critical load cases estimated in the loads process is used to size the more detailed structural model that will be used for performance evaluation. The shell-element structural models of wing, tails, and fuselage are separately generated, and coupled to form the complete model. The detailed static structural FE model for the XRF-1 for structural analysis in metallic design is shown in Fig. 4. It is sized based on critical loads calculated with the DMM. As the wing geometry and its position are subject to change during the optimization, wing spar positions and the tailplane positions may change, requiring an automatic update of the definition of the fuselage structure before structural coupling of fuselage and wings. System ribs (for landing gear, engine, flaps) are also adjusted during optimization. Fully-stressed design is used to size the structure. In each sizing iteration, wings/tails and fuselage are updated separately within the complete model, and then coupled again to produce a new complete model. The final sized model is sent to mission analysis, where it is used for a coupled static aeroelastic simulations of cruise flight points. Mission analysis can be performed by ordinary differential equation (ODE) integration over fuel burn, or in simplified manner, by using a single flight point and Breguet's range equation.

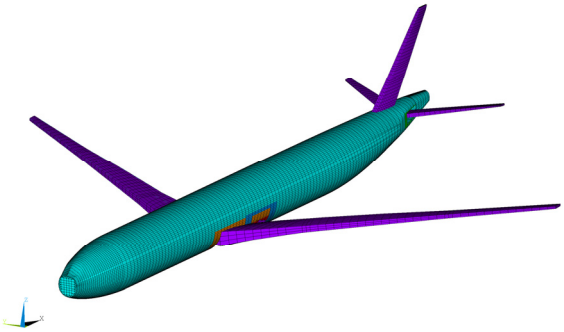

Fig. 4. Detailed structural XRF-1 model in metallic design

In terms of disciplinary tools, the finite element models of the wing and the empennage are created by DLR's structural model generator DELiS [13], while the fuselage model is created using DLR's TRAFUMO [15] model generator. Both tools generate fully parametric structural models based on CPACS input. The sub-models for fuselage and wing are coupled using consolidated interfaces. The structural solver is ANSYS. For isotropic materials, structural sizing with respect to strength and stability (local skin buckling) criteria is performed with variants of DLR's sizing tool S-BOT [16], which are implemented in ANSYS' internal programming language APDL. Sizing is performed based on input from the loads process in terms of critical SMT (shear, moment, torsion) loads, including maneuver and gust loads. Flow computations are performed with DLR's hybrid unstructured CFD code TAU [17] in RANS mode with the Spalart-Allmaras turbulence model. Coupling between TAU and ANSYS is performed using the FlowSimulator framework [5]. The performance of the engine is required for evaluating the objective function. An engine with suitable thrust requirements was designed using DLR's engine performance simulation tool GTlab [18]. The engine performance map and additional data were calculated offline and provided to the optimization process through CPACS. The value of fuel burn resulting from mission analysis is sent to the optimizer as the objective value, which then issues a new set of design variables, or detects convergence and stops the process.

4.1 Implementation aspects

As mentioned in the introduction, the disciplinary tools are linked into a single automatic optimization process with the help of the RCE framework. Using RCE, one can integrate disciplinary tools as standalone components, with defined inputs and outputs, and use a graphical workflow editor to create the process. The components are provided by a number of different servers, as well as by an HPC cluster. In a running workflow, RCE will transparently transmit the data between the components across the network.

Of particular interest is the run time of the single design analysis. Table 2 shows the run time broken down by subprocess, with the total being about 28 hours.

Subprocess	Run time	Of total
Preliminary design	1.3 [h]	5%
Loads	5.8 [h]	21%
Structure sizing	19 [h]	69%
Mission (Breguet)	1.3 [h]	5%
Total	27.4 [h]	100%

Table 2. Runtime breakdown of single design analysis

4.2 Optimization problem

The optimization problem used to demonstrate the gradient-free process starts from the previously described XRF-1 configuration as the baseline, and has the following properties.

The objective function is mission fuel burn. The mission profile is simplified to only the long-range cruise portion of 10500 km, flown at Mach number 0.83, and three altitude segments, at 11000 m, 11500 m, and 12000 m. To save on the run time, however, continuous cruise-climb is assumed, so that fuel burn can be extracted from a single mission point evaluation using the Breguet range equation.

All the design constraints are satisfied within the single design analysis, so that the top optimizer sees an unconstrained optimization problem. The observed constraints are constant wing area and wing root chord (fixed through choice of parametrization), stability margin (enforced by tail sizing in preliminary design), landing/takeoff distance (only roughly constant, thanks to fixed wing area), and strength and buckling failure criteria (enforced by fully-stressed design). In each design analysis, about 1,500 load cases are examined, and 50 to 60 selected as critical for structural sizing.

The design parametrization is formulated for the wing only. The wing consists of three trapezoidal segments. Leading edge sweep is kept constant across the segments, i.e. leading edge is straight. Dependencies between planform parameters are formulated such that the wing area and root chord are independent parameters, and can be kept constant (the reason for constant chord is to fit the fixed fuselage belly geometry). With this in mind, Table 3 shows the list of 9 selected design parameters, consisting of 7 planform parameters and 2 section parameters. Numbers to parameters denote spanwise positions of planform breaks, from 1 at wing root to 4 at tip.

Parameter	Base.	Min.	Max.
Aspect ratio	9.2	7	12
Sweep [°]	32	24	40
Taper ratio 2-3	0.59	0.20	0.80
Taper ratio 3-4	0.55	0.20	0.80
Twist 2 [°]	0.5	-6	6
Twist 3 [°]	1.0	-6	6
Twist 4 [°]	-2.0	-6	6
Section 2 thickness change [%]	0	-25	25
Section 4 thickness change [%]	0	-25	25

Table 3. Selected design parameters

The employed aerodynamic CFD mesh has 2.2 million points, and the structural FEM model has about 100,000 degrees of freedom. For the fully-stressed design, the wing, tails, and fuselage are segmented into a total of 1001 sizing regions.

4.3 Results of MDO

Given the long run time of a single design analysis, on the order of two days, at the time of this writing the optimization is not yet complete. However, one modified design has been found so far to yield an improvement over the baseline. This modified design has aspect ratio

increased from 9.2 to 10.2, which resulted in reduction of drag by 2 counts, and, perhaps surprisingly, no increase in structural mass (change was below 100 [kg] convergence criterion for loads and sizing subprocesses), giving fuel burn reduction of 1%. The drag reduction is also at first suspiciously low for the given aspect ratio increase, as according to the analytic elliptic wing formula, drag should have been reduced by at least 8 counts.

The cause of this curious improvement lies in the multidisciplinary tradeoff. Fig. 5 shows the geometries of the baseline and modified designs. It can be seen that the modified wing has higher span and is moved somewhat forward. The modified horizontal tail is a little bit smaller, having about 3% less area, which is difficult to see in the figure.

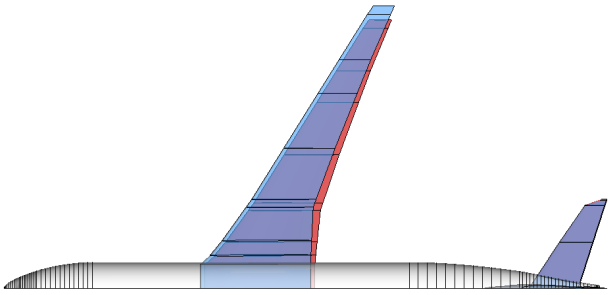

Fig. 5. Baseline (red) and modified (blue) design

This has caused the following chain of effects. Critical load on the wing became smaller, as shown by the integrated bending moment in Fig. 6, because of the reduced downforce on horizontal tail needed for balance.

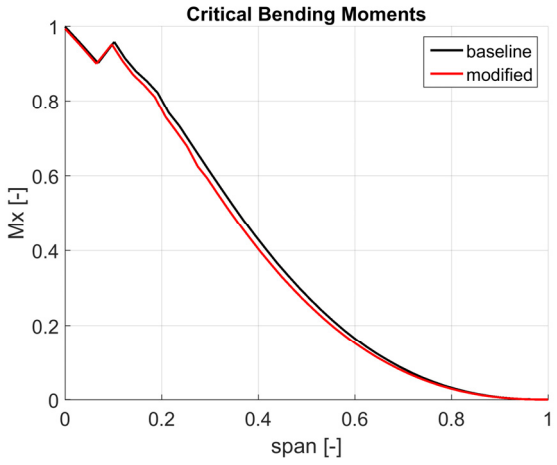

Fig. 6. Integrated critical wing bending moment for baseline and modified designs, normalized to baseline

Reduction in critical load in turn caused reduction of wing mass in outer wing per unit span, as illustrated by wing skin mass in Fig. 7. Since the modified design has higher span, the overall wing mass remained the same between the two designs.

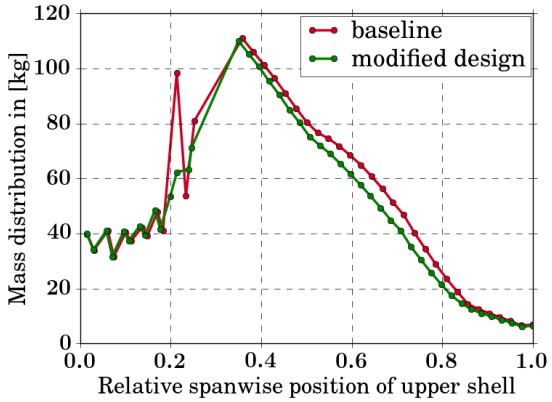

Fig. 7. Upper wing skin mass distribution for baseline and modified designs. The peak at a spanwise location 0.2 for the baseline is an artifact of automatic rib placement at the transition from ribs oriented in direction of flight (inboard) to spar-normal ribs (outboard wing).

Lower mass per unit span means lower wing stiffness, which resulted in higher wing bending and thus higher effective section twist towards the tip in the modified design. Higher twist caused the spanwise load distribution in cruise flight to move further away from the elliptic compared to baseline, as seen in Fig. 8, eating away part of the aspect ratio advantage for induced drag. Furthermore, wing sections no longer operate exactly at baseline design conditions, giving a small increase in shock strength, as shown for one section in Fig. 9, further undermining the gains in the induced drag.

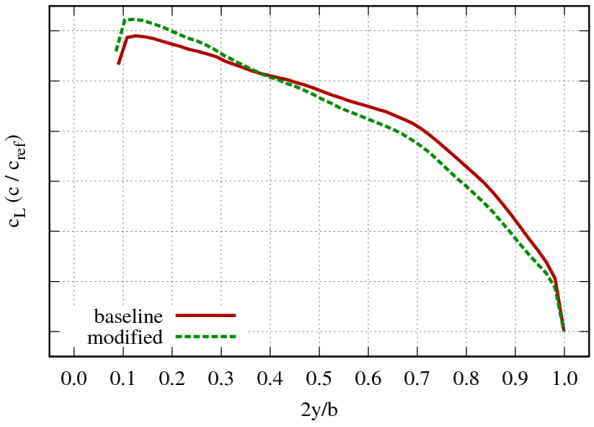

Fig. 8. Spanwise load distribution for baseline and modified designs

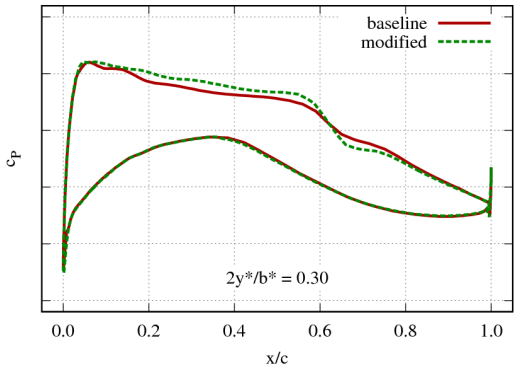

Fig. 9. Section pressure distribution at a spanwise location 2y*/b*=0.3 for baseline and modified design. y*, b* indicate spanwise position y defined between wing root and tip, instead of between centerline and tip, used due to different wing spans b of the two designs.

As the optimization continues, further improvement can be expected, for example as the section twist parameters get modified in a way to cancel out the observed shock increase.

5 Gradient-Free High-Fidelity MDO

Parallel to the ongoing multi-level MDO, an MDO using the high-fidelity detailed-level tools only was performed. This allowed us to demonstrate the technical feasibility of a less complex but integrated MDO process distributed across different DLR institutes earlier. This optimization was performed for a simplified XRF-1, consisting of wing and fuselage, using again the subplex algorithm. High-fidelity CFD calculations were used for the wing/fuselage aerodynamics, coupled with a finite element analysis of the wing structure to determine the static aeroelastic equilibrium. In addition, the wing structure was sized using two predefined load cases (2.5g and -1g at Mach 0.83 and 6000m alt.) for each optimization step, instead of employing the full loads process. The wing was parameterized using five geometric parameters, with planform area and root chord also kept constant. Fig. 10 and Fig. 11 show results of an optimization of the block fuel mass. The fuel consumption was reduced by 3.6%. Two optimizations were performed, one using ODE mission analysis for a 3-step cruise climb, and one using the Breguet equation. The runtime of single design evaluation with ODE approach was 18 hours, and with Breguet approach 12 hours. The complete optimization took 45 and 30 days to complete, respectively. A total of 192 cores of an HPC cluster were used for high-fidelity CFD-CSM computations, and a single workstation was used for structural sizing.

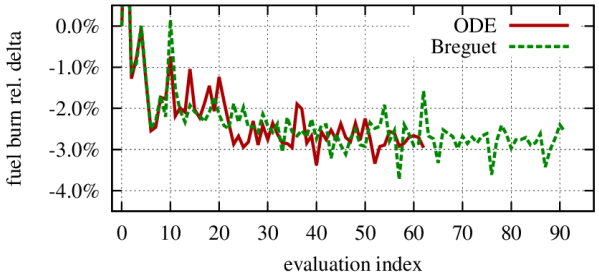

Fig. 10. Optimization history relative to baseline for ODE-based and Breguet-based fuel-burn evaluation [19]

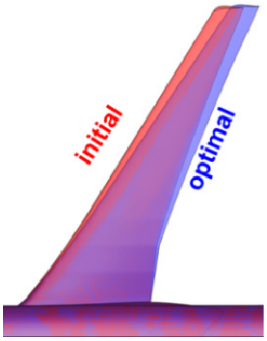

Fig. 11. Result of hi-fi MDO of XRF-1 wing/fuselage configuration: initial and optimized wing shape [19]

The absolute values of the fuel burn differed between these two optimizations, but the relative reduction of fuel burn, as well as the optimal values of design parameters, were practically the same. This is further illustrated by the same lift-to-drag polars of both designs, shown in Fig. 12. This result motivated the use of Breguet's range equation for the more expensive multi-level MDO in the previous section. More details on this gradient-free high-fidelity MDO can be found in [19].

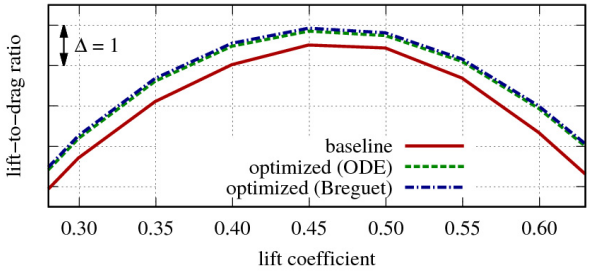

Fig. 12. Comparison of lift-to-drag polars between the baseline and two optimized designs [19]

6 Gradient-Based High-Fidelity MDO

As it was clear from the beginning that a sequential gradient-free MDO process will require very long run times, a gradient-based process with limited scope was developed in parallel to improve the overall efficiency of the MDO. To deal with complexity, it was implemented for high-fidelity aero-structural optimization at the detailed level only, but also because not all tools of the gradient-free multi-level process readily provide gradients. Assuming that the computation of the available gradients is efficient, these algorithms make it possible to employ a large number of design parameters.

A general gradient-based aero-structural optimization can be represented via the flow chart shown in Fig. 13. As depicted, after updating the design variables both the CFD and the CSM model need to be generated. In this study the design variables that control the outer shape were chosen to be freeform deformation (FFD) parameters, and the design variables that define the structure model are structural thicknesses of the wings skin, ribs and spars.

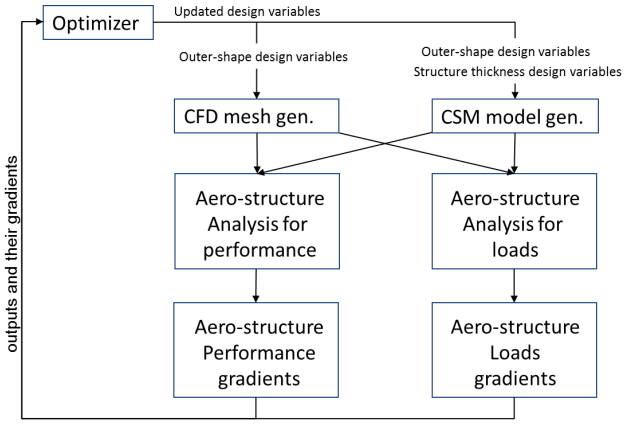

Fig. 13. General flow chart of a gradient-based aerostructural optimization

Instead of generating the CFD model for each update of design variables, the FFD parameters were applied directly on the CFD mesh to perform an efficient mesh deformation. The FFD parameters change only the wing profile shapes with constant planform and are set in a way to guarantee a constant leading edge radius, which is important for the installation of high-lift devices. This FFD setting included 360 design variables. The CSM finite element model was regenerated for each update in structural thicknesses via the model generator DELiS by taking in 348 structural thicknesses as input.

After generating the models, two parallel types of analysis take place; the performance analysis block which computes the aerodynamic coefficients and the loads analysis block which computes the wing mass and checks if all the structure failure criteria are satisfied. To compute the aero-structure states in both analysis blocks, high-fidelity RANS solver (DLR-TAU) was coupled with a linear-elasticity based FEM commercial solver (ANSYS Mechanical).

On the performance side, five points were optimized, including the cruise design point (C_L=0.5, Ma=0.83) with the highest weighting factor of 0.4, and four points around it (C_L±0.03, Ma±0.02) each with a weighting factor of 0.15. On the loads side a study was performed before the optimization to identify the critical aerodynamic maneuver load cases.
In the literature, usually several maneuver load cases are predefined to size the wing structure without making sure that these load cases are actually critical to the wing structure. This results in a structure that will most probably fail under the critical maneuver load cases. For this reason, it was decided in this study to compute the whole Mach-altitude envelope for five critical mass cases in order to decide what the critical aerodynamic load cases are for the baseline configuration.

The five mass cases considered were the operating empty mass, two maximum take-off mass cases, once with maximum fuel and once with maximum payload, a mass case with zero payload and maximum fuel, and a mass case with zero fuel and maximum payload. After computing the Mach-altitude envelope for the five mass cases, the loads were sent to the sizing tool S-BOT, which can tell the designer what the critical load cases are.

The process computed loads at intervals in Mach of 0.02 and steps in altitude of 1000 meter for two load factors; -1g and 2.5g. A total of 400 load cases were considered. Since this process is very expensive, POD-based reduced order models (ROMs) [20] were employed

using DLR's SMARTy toolbox to explore with continuity the parameter space at in-between altitudes and to identify additional critical load cases, increasing the efficiency of the process. By means of the ROMs, 360 additional predictions for two mass cases were computed. Fig. 14 shows the complete aerodynamic load case identification process.

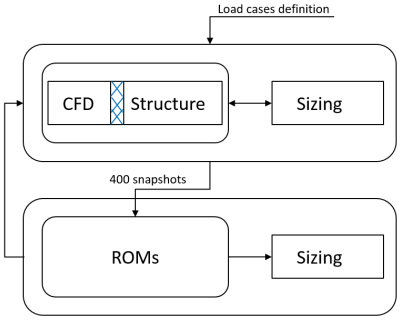

Fig. 14. The load case identification process

Fig. 15 illustrates the Mach-altitude envelope that was computed for one of the mass cases, with the usual dive and stall speed limits, but also with flow separation limits, which could be found due to use of a RANS solver. It can be seen that sizing-critical load cases are not on the dive and stall limits, but rather clustered around the flow separation limits. The cause for this is that flow separation starts from the outer part of the wing, thus shifting the load distribution towards the wing root and relieving the wing structure.

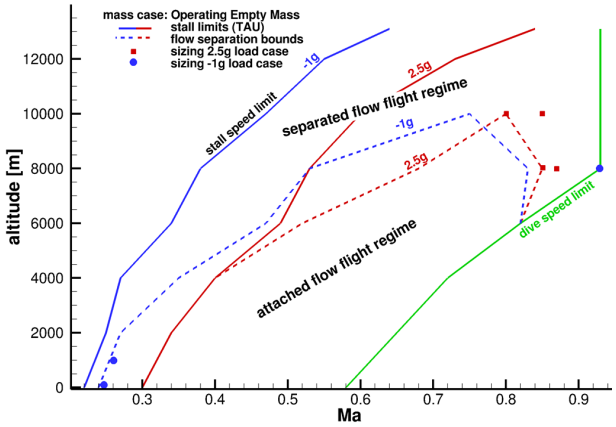

Fig. 15. Mach-altitude envelope of load cases for operating empty mass case

The load case identification process resulted in 12 critical load cases, 7 of them were sizing around 95% of the wing. To decrease the computational effort during the aerostructural optimization, only these 7 load cases were considered and computed for every update in the design variables. It is worth mentioning here that the initial CSM wing is the one sized with S-BOT under the identified critical load cases.

After computing the aerostructural states, the gradients of all objectives and constraints with respect to all design variables need to be computed and forwarded to the optimizer to perform a search for a better design. Computing all these gradients is not feasible with the current computational power in acceptable time frame. The reason is that the adjoint approach cannot handle thousands of constraints as in the structure problem and the finite differences approach cannot handle solving the nonlinear coupled system as many times as the number of design variables, which is 708 in this study.

A typical compromise here is to aggregate the structural constraints [21] from thousands to tens, and then employ the coupled adjoint approach. This adds some conservatism to the structure sub-optimization problem but provides the gradients efficiently.

Another compromise, which is used in this study, is to identify at the beginning of the optimization the so-called optimization-driving gradients and neglect computing the other gradients. The nature of the design variables can be such that the outer shape parameters have higher effect on the aerodynamics than on the structure and the structural thicknesses have higher effect on the structure of the wing than on the aerodynamic performance. Having no outer shape parameters that affect the wing planform, for example, makes the sensitivity of structural mass with respect to the outer shape parameters much smaller than that with respect to the structural thicknesses. This is illustrated by Fig. 16 for aerodynamic drag and mass gradients (gradients of structural constraints follow a similar pattern).

The FSQP algorithm [22] was used to drive the optimization. SQP (sequential quadratic programming) type algorithms are typically used in contexts of large number of constraints. In FSQP in particular, F stands for *feasible*: only those designs which do not violate any constraints will be accepted. This is important in the present case, because, due to the neglected elements of the gradient, a non-

feasible SQP algorithm may fail to satisfy all the constraints, or take too many iterations to do so. With the FSQP algorithm, on the other hand, an inexact gradient will result in stopping before the true optimum has been reached, but the final design will be guaranteed to be feasible and might have a sufficient improvement in the objective over the initial design.

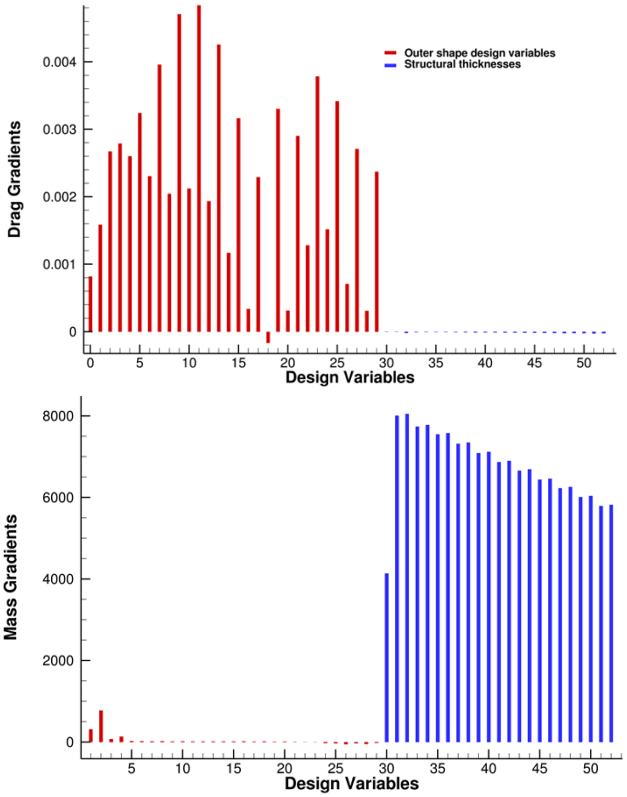

Fig. 16. Drag (top) and mass (bottom) gradients with respect to aerodynamic and structural design variables

This is indeed the result that was reached in the present case, as illustrated by the optimization convergence plot in Fig. 17. The objective is the range coefficient, which is equal to the product of the lift-to-drag ratio and inverse of the mass coefficient. The objective was increased by about 6% from the baseline, which was achieved both by increase in lift-to-drag ratio and by decrease in the mass coefficient. The total run time for this optimization was 80 hours, using 96 computing cores of an HPC cluster. In total 230 CFD-CSM simulations (load cases and performance cases) were performed.

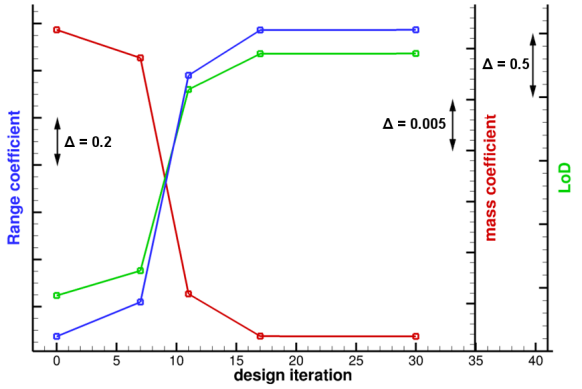

Fig. 17. Gradient-based optimization convergence. Only accepted designs after each line search are shown.

The comparison of off-design performance of the optimized and baseline designs is given by the aeroelastic lift-to-drag polar in Fig. 18 at design Mach number. There is a small peak in the objective improvement at the cruise design point, due to its higher weight of 0.40 in the multi-point objective, but not at the expense of the nearby off-design points, which are improved over the baseline as well.

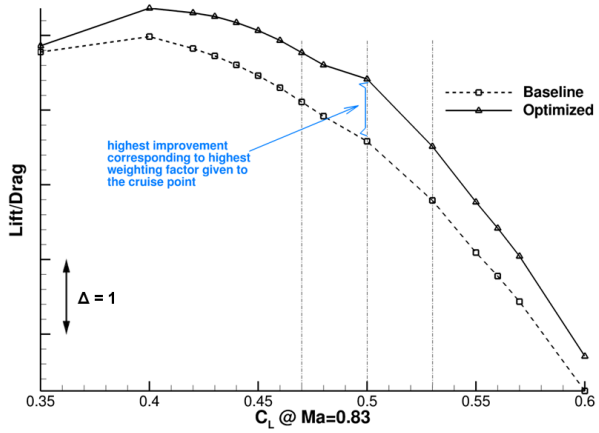

Fig. 18. Comparison of aeroelastic polars of baseline and optimized designs

7 Conclusions

DLR has developed a collaborative MDO platform based on DLR standards and more than 40 established disciplinary tools. A multi-level MDO architecture has been implemented, including an overall aircraft synthesis tool chain, an automatic loads process based on mid-fidelity aerodynamics to identify configuration-specific load cases, aerodynamic performance computations for the aeroelastic aircraft with automatic hybrid unstructured meshing for

RANS-based CFD, improved structural modeling, structural sizing of wing, fuselage and tail, and mission analysis. The MDO platform reached initial operational capability as demonstrated by optimizing a generic wide-body transport aircraft configuration. The potential of gradient-based MDO in terms of overall efficiency has been demonstrated based on high-fidelity methods and will be used as a motivation to extend the multi-level MDO process to make use of gradients.

Acknowledgements

The first author has chosen to list one co-author for every DLR institute involved in this project; however, this work is the collaborative effort of the following 38 colleagues from eight different DLR institutes at six different sites, who all contributed over time with various levels of involvement. Aside from those listed as authors the following people also made significant contributions:
S. Keye, M. Kruse, T. Wunderlich, G. Einarsson, N. Banavara, N. Karcher, T. Franz, M. Schulze, A. Schuster, S. Dähne, T. Bach, P. D. Ciampa, T. Zill, M. Petsch, M. Leitner, M. Verveld, T. Stollenwerk, S. Zur, D. Seider, J. Brezillon, O. Brodersen, J. Himisch, T. Gerhold, A. Ronzheimer, C. Liersch, T. Wille, D. Kohlgrüber, N. Kroll.

References

[1] Liersch, C, Hepperle, M. A distributed toolbox for multidisciplinary preliminary aircraft design. *CEAS Aeronautical Journal*, Vol. 2, No. 1-4, pp 57-68. Springer, 2011.

[2] Nagel, B, Zill, T, Moerland, E, Böhnke, D. Virtual Aircraft Multidisciplinary Analysis and Design Processes - Lessons Learned from the Collaborative Design Project VAMP. *Proc. 4th CEAS Air and Space Conference*, Linköping, Schweden, 2013.

[3] Ronzheimer, A, Natterer, F.J., Brezillon, J. Aircraft Wing Optimization Using High Fidelity Closely Coupled CFD and CSM Methods. *AIAA-Paper 2010-9078*. 13th AIAA/ISSMO Multidisciplinary Analysis Optimization Conference, 2010.

[4] Kroll, N, Abu-Zurayk, M, Dimitrov, D, Franz, T, Führer, T, Gerhold, T, Görtz, S, Heinrich, R, Ilić, Č, Jepsen, J, Jägersküpper, J, Kruse, M, Krumbein, A, Langer, S, Liu, D, Liepelt, R, Reimer, L, Ritter, M, Schwöppe, A, Scherer, J, Spiering, F, Thormann, R, Togiti, V, Vollmer, D, Wendisch, J-H. DLR Project Digital-X – Towards Virtual Aircraft Design and Flight Testing based on High-Fidelity Methods. *CEAS Aeronautical Journal*, Vol. 7, No. 1, pp 3–27, March 2016.

[5] Meinel, M, Einarsson, G. The FlowSimulator framework for massively parallel CFD applications, *Proc. PARA 2010*. PARA2010, 6.-9. Juni 2010, Reykjavik, Island, 2010.

[6] Seider, D, Zur, S, Flink, J, Mischke, R, Seebach, O. RCE – Distributed, Workflow-driven Integration Environment, *Proc. EclipseCon Europe 2013*, 29 - 31 Oct 2013, Ludwigshafen, 2013.

[7] Rizzi, A, Zhang, M, Nagel, B, Böhnke, D, Saquet P. Towards a Unified Framework using CPACS for Geometry Management in Aircraft Design, *AIAA Paper 2012-0549*, AIAA Aerospace Sciences Meeting, Nashville, USA, 2012.

[8] Ciampa, P, Nagel, B, La Rocca, G. Preliminary Design for Flexible Aircraft in a Collaborative Environment. *Proc. 4th CEAS Air & Space Conference*, 16-19 Sep 2013, Linköping, Sweden, 2013.

[9] Jepsen, J, Ciampa, P, Nagel, B. Design of a common library to simplify the implementation of aircraft studies in CPACS. *Proc. 64. Deutscher Luft- und Raumfahrtkongress (DLRK 2015)*, 22.-24. September 2015, Rostock, Germany, 2015.

[10] Liepelt, R, Handojo, V, Klimmek, T. Aeroelastic Analysis Modelling Process to Predict the Critical Loads in an MDO Environment. *Proc. IFASD 2015* - International Forum on Aeroelasticity and Structural Dynamics, 2015.

[11] Kier, T, Looye, G, Scharpenberg, M, Reijerkerk, M. Process, Methods and Tools for Flexible Aircraft Flight Dynamics Model Integration. *Proc. IFASD 2007* - International Forum on Aeroelasticity and Structural Dynamics, 2007.

[12] Kier, T, Looye, G. Unifying Manoeuvre and Gust Loads Analysis. *Proceedings IFASD 2009* - International Forum on Aeroelasticity and Structural Dynamics, 2009.

[13] Führer, T., Willberg, C., Freund, S., Heinecke, F. "Automated model generation and sizing of aircraft structures," *Aircraft Engineering and Aerospace Technology*, Vol. 88, No. 2, pp 268 – 276, 2016.

[14] Bach, T, Führer, T, Willberg, C, Dähne, S. Automated sizing of a composite wing for the usage within a multidisciplinary design process. *Aircraft Engineering and Aerospace Technology*, Vol. 88, No. 2, pp 303 – 310, 2016.

[15] Scherer, J, Kohlgrüber, D. Fuselage Structures within the CPACS Data Format. *Aircraft Engineering and Aerospace Technology*, Vol. 88, No. 2, p. 294-302, 2016.

[16] Scherer, J, Kohlgrüber, D, Dorbath, F, Sorour, M. A finite element based tool chain for structural sizing of transport aircraft in preliminary aircraft design. *Proc. 62. Deutscher Luft- und Raumfahrtkongress (DLRK 2013)*, Stuttgart, Germany, 2013.

[17] Schwamborn, D, Gerhold, T, Heinrich, R. The DLR TAU code: recent applications in research and industry. *Proc. European Conference on*

Computational Fluid Dynamics, ECCOMAS CDF 2006, Delft, The Netherland, 2006.

[18] Becker, R, Reitenbach, S, Klein, C, Otten, T, Nauroz, M, Siggel, M. An Integrated Method for Propulsion System Conceptual Design. *Proc. ASME Gas Turbine Technical Congress and Exposition*. ASME Turbo Expo 2015, 15.-19. June 2015, Montréal, Canada, 2015.

[19] Ilić, Č, Führer, T, Banavara, N, Abu-Zurayk, M, Einarsson, G, Kruse, M, Himisch, J, Seider, D, Becker, R. Comparison of Breguet and ODE evaluation of the cruise mission segment in the context of high-fidelity aircraft MDO. *Notes on Numerical Fluid Mechanics and Multidisciplinary Design*, Vol. 132: New Results in Numerical and Experimental Fluid Mechanics X Contributions to the 19th STAB/DGLR Symposium Munich, Germany, 2014, Springer, 2016.

[20] Zimmermann, R, Görtz, S. Non Linear Reduced Order Models for Steady Aerodynamics. *Procedia Computer Science*, Vol. 1, Issue 1, pp. 165–174, ICCS 2010, May 2010,.

[21] Lambe, A, Kennedy, G, Martins, J. An evaluation of constraint aggregation strategies for wing box mass minimization. *Struct Multidisc Optim*, pp 1-21, Springer, 2016.

[22] Zhou, J, Tits, A, Lawrence, C. User's Guide for FFSQP Version 3.7., 1997.

Contact Author Email Address

For further information please send an email to the lead author: stefan.goertz@dlr.de

Copyright Statement